BNL-98552-2012-CP

HIGH RADIATION ENVIRONMENT NUCLEAR FRAGMENT SEPARATOR DIPOLE MAGNET*

S.A. Kahn#, Muons, Inc., Batavia, IL 60510, U.S.A.
R.C. Gupta, BNL, Upton, NY 11973, U.S.A.

Abstract

Magnets in the fragment separator region of the Facility for Rare Isotope Beams (FRIB) would be subjected to extremely high radiation and heat loads. Critical elements of FRIB are the dipole magnets which select the desired isotopes. Since conventional NiTi and Nb_3Sn superconductors generally operate at ~4.5 K, the removal of the high heat load generated in these magnets with these superconductors would be difficult. The coils for these magnets must accommodate the large curvature from the 30° bend that the magnet subtends. High temperature superconductor (HTS) has been shown to be radiation resistant and can operate in the 30-50 K temperature range where heat removal is an order of magnitude more efficient than at 4.5 K. Furthermore these dipole magnets must be removable remotely for servicing because of the extremely high radiation environment. This paper will describe the magnetic and conceptual design of these magnets.

INTRODUCTION

The Facility for Rare Isotope Beams (FRIB) will provide isotope beams for physics research with intensities not available elsewhere. Large quantities of the various isotopes are produced when a high power linac beam hits the target. The dipole and quadrupole magnets in the fragment separator, which select the rare nuclides from the multitude of secondary fragments, would be subject to extremely high radiation and high field loads [1]. This paper is concerned with the dipole magnet.. The magnet has a 4 m bending radius and subtends a bend angle of 30°. The magnetic properties of are specified in Table 1. Because of the large heat load from radiation High Temperature Superconductor (HTS) is chosen for the coils. The basic design is a sector superferric magnet where the coils magnetize the iron yoke and the iron design dominates the field quality. As in the case of quadrupoles in the fragment separator region [2], HTS is an ideal conductor choice for operating the dipoles at 40 K where the heat capacity of the coolant is large enough to remove the heat from the coils. Figure 1 shows a sketch of the sector bend magnet where only half of the upper half of the iron return yoke is shown.*

*Work supported by DOE-STTR grant DE-SC0006273
#kahn@muonsinc.com

MAGNET DESIGN

The magnetic pole which determines the field shape of the magnet is curved to follow the beam trajectory. The YBCO conductor used for the coils that are placed around the pole is only available in tape form. Winding the tape conductor on the inner surface of the pole where the curvature is negative produces some difficulties since the conductor turns will tend to unwind during the process. We describe in another paper [3] a study where we develop and test a technique to wind a coil with negative curvature for this magnet.

Although Bi-2212 conductor could be used for this application, we have chosen YBCO because it is currently available in the large quantity that is required for this magnet. The magnet will be wound with 12 mm wide YBCO tape that will be interleaved with stainless steel tape to act as a radiation resistant insulator which also provides strength to the coil. This will avoid the use of organic insulations which are often subject to radiation damage. Epoxy will only be used on the edges of the conductor as an assembly aid during the winding process. In order to achieve the desired 2 T field the upper and lower coils must carry 256K amp-turns in this design.

Table 1: Parameters Describing the Magnetic Properties of the Fragment Separator Dipole Magnet

Parameter	Value
Bending Radius	4 m
Bend Angle	30°
Effective Length along Design Trajectory	2.094 m
Max. Dipole Field	2.0 T
Variable Field Range	0 to 2.0 T
Field Non-Uniformity in Good Field Region	<0.7% for fields between 0.5 T to 2.0 T
Uniform Field Width in Bend Plane	0.3 m
Uniform Field in Non-Bend Plane	0.2 m

Copyright © 2012 by IEEE – cc Creative Commons Attribution 3.0 (CC BY 3.0) — cc Creative Commons Attribution 3.0 (CC BY 3.0)

ISBN 978-3-95450-115-1

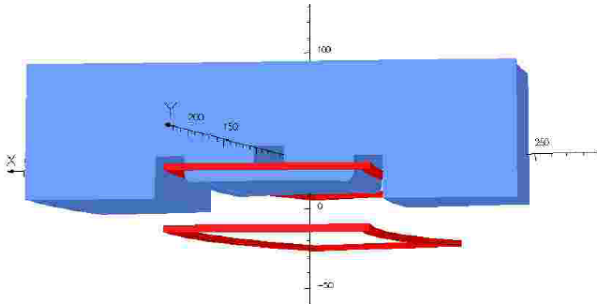

Figure 1: 3D sketch of the sector dipole magnet. One quarter of the iron return yoke is shown in the figure.

TWO DIMENSIONAL MODEL

Because of the curvature of the magnet the field in the 2D cross section is expected to have a slight left-to-right asymmetry. This can be simulated by sweeping the 2D r-z cross section along a closed circular arc with the beam orbit radius. Figure 2 illustrates the magnet r-z section. The field error, ΔB/B, should be less than 0.7% for the field range from 0.7 to 2.0 T. This is achieved by controlling the magnetization in the return yoke. Figure 3 shows the relative permeability in the iron. The iron on the smaller radius inner side shows more saturation than the larger radius outer side. The rectangular hole in the pole is place there to effectively control the saturation.

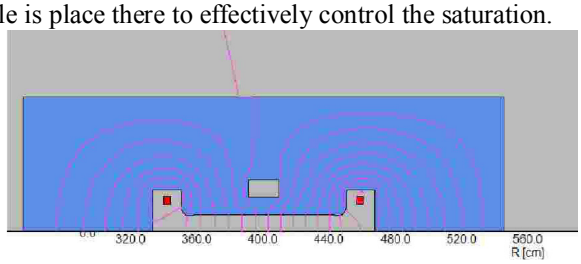

Figure 2: Sketch of the r-z cross section of the FRIB bend magnet. The blue represents the iron yoke and the red represents the coils. Field lines are superimposed and show a slight asymmetry due to the magnet curvature.

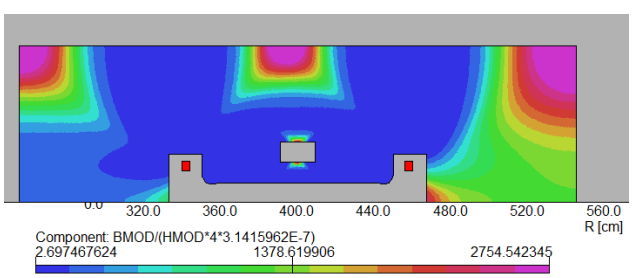

Figure 3: Relative permeability of the iron yoke is shown.

In Fig. 4 ΔB/B as a function of x in the aperture is shown for various field excitations. The field error is less than 0.7% for all values of B_0 in the good field region of ±30 cm. The coils will feel substantial Lorentz forces when the magnet is fully energized. Table 2 shows the coil forces at the 2.0 T operating field and at the 2.2 T maximum design field. These forces are large enough to require mechanical support to the coils. The tensile strain on the conductor is estimated to be less than 0.15% which is safely below the strain limit.

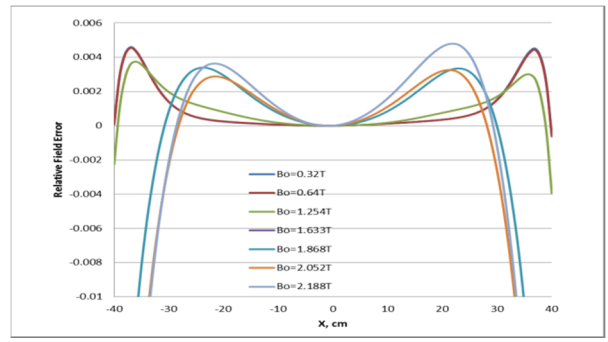

Figure 4: The relative error ΔB/B as a function of position in the aperture. Curves are shown for different central fields ranging from 0.32 T to 2.188 T.

Table 2: Lorentz Forces on the Coil

Field	Coil	F_{radial}	$F_{vertical}$
Tesla		nt	nt
2.0	Outer	289533	252403
	Inner	-194879	194313
2.2	Outer	400714	269127
	Inner	-261610	211187

COIL CONFIGURATIONS

The two coil configurations that are being considered for this magnet are shown in Fig. 5. The left diagram shows coils that are wound with a negative curvature which poses difficulties during winding as the conductor will tend to unwind. The right diagram avoids the negative curvature complications with a straight conductor segment. The iron return yoke is also modified to accommodate the conductor. This however breaks the r-z symmetry. These two configurations were compared using the Tosca 3-D EM finite element program [4]. Figure 6 shows a contour plot of B_z on the mid-plane for the two coil configurations.

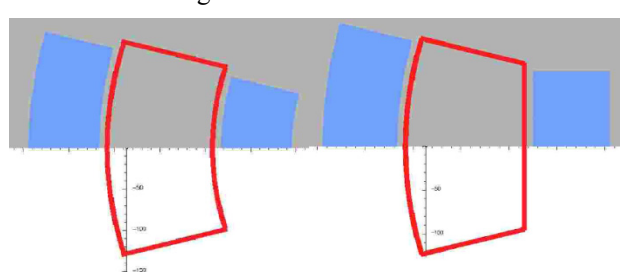

Figure 5: Two coil configurations examined. The left diagram uses a curved inner radius coil which was wound with negative curvature. The right diagram uses straight conductor.

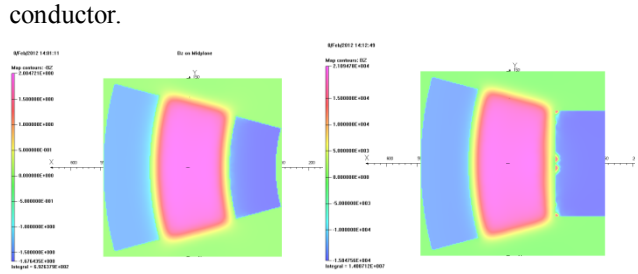

Figure 6: Contour plot of B_z on the magnet mid-plane for the two coil configurations.

Copyright © 2012 by IEEE – cc Creative Commons Attribution 3.0 (CC BY 3.0) — cc Creative Commons Attribution 3.0 (CC BY 3.0)

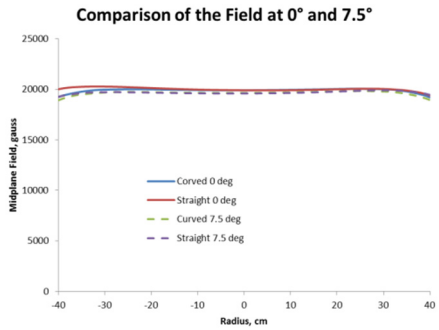

Figure 7: Comparison of the field in a cross section at 0° and at 7.5°. Curves are shown for the straight and curved configurations.

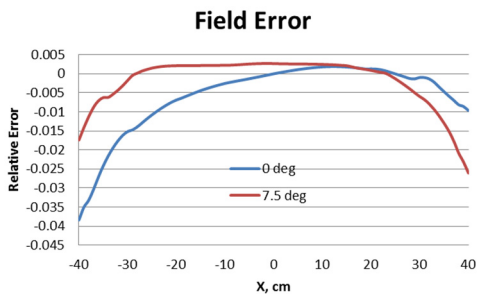

Figure 8: Fractional difference in field between the straight and curved inner segment configurations. The blue (red) curve shows the field difference in a transverse plane at 0° (7.5°).

The field along the mid-plane in a transverse plane to the reference path is shown in Fig. 7 for the straight and curved inner coil segment. The figure shows fields at the 0° magnet center and at the 7.5° magnet quarter point. Figure 8 shows the relative difference between the two configurations. The difference is largest at 0° which is expected. The maximum difference in the good field region is 1.5%. The magnetic pole can be shaped to further reduce this small field error, if necessary. The field along the reference trajectory is shown for the two configurations in Fig. 9. Figure 10 shows the relative difference between the configurations along the reference path (4 m radius) and along paths 20 cm closer (3.8 m) and farther (4.2 m) from the reference path. The abscissa for that plot is angle with ±15° representing the magnet end. The greatest deviation is at the magnet ends. The curved and straight fields are normalized so that the field at 0° is the same for the two configurations.

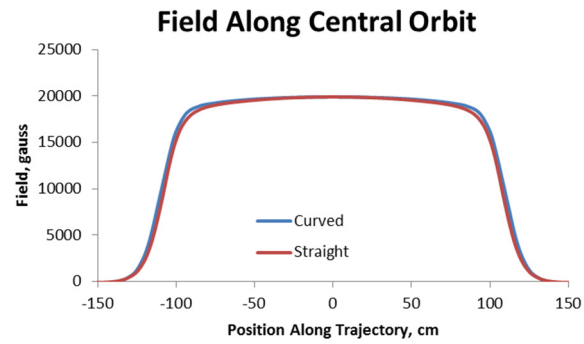

Figure 9: Field along the reference trajectory as a function path position.

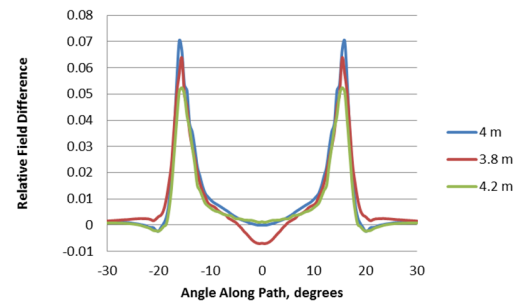

Figure 10: The $\Delta B/B_0$ as a function of magnet angle along the reference path and ±20 cm closer and farther from the path.

CONCLUSIONS

The magnet design using HTS offer significant advantages over conventional low temperature superconductor when used in the high radiation environment of FRIB. We have analyzed the magnetic design for a dipole magnet using YBCO tape. Two coil geometries were examined. The coil configuration with the straight inner segment is easier to fabricate (and hence preferred) than the configuration with a curved inner segment that requires the magnet to be wound with a negative curvature segment. The difference in field between these two configurations is relative small and the magnetic pole can be modified to correct for these differences.

ACKNOWLEDGMENT

The authors would like to thank Al Zeller from MSU for his guidance and feedback on the dipole design parameters.

REFERENCES

[1] A. Zeller et al., "Radiation Resistive Magnets for the RIA Fragment Separator", Particle Accelerator Conference, Knoxville, TN, USA (2005).
[2] R. Gupta, et al., "Second Generation HTS Quadrupole for FRIB", ASC2010 4LZ-05, 2010.
[3] S. Kahn et al., "Curved Test Coil for FRIB Fragment Separator Dipole", submitted to IPAC12.
[4] TOSCA 3D Electromagnetic Finite Element Program from Cobham Technical Services.

Copyright © 2012 by IEEE – cc Creative Commons Attribution 3.0 (CC BY 3.0) — cc Creative Commons Attribution 3.0 (CC BY 3.0)

ISBN 978-3-95450-115-1